Physisorption of functionalized gold nanoparticles on AlGaN/GaN high electron mobility transistors for sensing applications

M. S. Makowski,[1,2] S. Kim,[3] M. Gaillard,[4] D. Janes,[3] M. J. Manfra,[3,5] I. Bryan,[6] Z. Sitar,[6] C. Arellano,[7] J. Xie,[8] R. Collazo,[6] and A. Ivanisevic[6,9,a)]

[1]*Weldon School of Biomedical Engineering, Purdue University, West Lafayette, Indiana 47907, USA*
[2]*Indiana University School of Medicine, Indianapolis, Indiana 46202, USA*
[3]*School of Electrical and Computer Engineering, Purdue University, West Lafayette, Indiana 47907, USA*
[4]*Department of Bioengineering, Clemson University, Clemson, South Carolina 29634, USA*
[5]*Department of Physics and School of Materials Engineering, Purdue University, West Lafayette, Indiana 47907, USA*
[6]*Department of Materials Science and Engineering, North Carolina State University, Raleigh, North Carolina 27695, USA*
[7]*Department of Statistics, North Carolina State University, Raleigh, North Carolina 27695, USA*
[8]*HexaTech, Inc., 991 Aviation Pkwy, Suite 800, Morrisville, North Carolina 27560, USA*
[9]*Joint Department of Biomedical Engineering, North Carolina State University, University of North Carolina, Raleigh, North Carolina 27695, USA*

(Received 26 November 2012; accepted 29 January 2013; published online 19 February 2013)

AlGaN/GaN high electron mobility transistors (HEMTs) were used to measure electrical characteristics of physisorbed gold nanoparticles (Au NPs) functionalized with alkanethiols with a terminal methyl, amine, or carboxyl functional group. Additional alkanethiol was physisorbed onto the NP treated devices to distinguish between the effects of the Au NPs and alkanethiols on HEMT operation. Scanning Kelvin probe microscopy and electrical measurements were used to characterize the treatment effects. The HEMTs were operated near threshold voltage due to the greatest sensitivity in this region. The Au NP/HEMT system electrically detected functional group differences on adsorbed NPs which is pertinent to biosensor applications. © *2013 American Institute of Physics*. [http://dx.doi.org/10.1063/1.4791788]

With the need for rapid detection of biomolecular analytes in the life sciences and medicine, the research community has made great progress in developing microscale and nanoscale sensors for many biological applications.[1,2] One promising biosensor structure is the AlGaN/GaN high electron mobility transistor (HEMT) due to its chemical stability,[2] electrical stability in ionic solutions,[3] biocompatibility,[4,5] and high sensitivity to adsorbed surface charges.[2] These devices have been used for many biomedical and life sciences applications including detection of proteins,[6] DNA,[7] pathogens,[8] and cellular signals.[9] A two dimensional electron gas (2DEG) is formed at the interface between the AlGaN and GaN layers due to piezoelectric polarization and spontaneous polarization that is sensitive to adsorbed surface charges.[2] Binding of a charged analyte near the gate area of a HEMT biosensor changes the surface potential at the gate that modulates the conductance of the 2DEG charge carrier channel and results in a measureable change in electrical current through the device.[2,10]

A critical step in biosensor fabrication is the binding of biological receptors to the device surface that are specific to the analyte of interest. Linker molecules are used to form an interface between the underlying inorganic device and the receptors. Previously demonstrated methods used to bind linkers to the gate area of AlGaN/GaN HEMTs include patterning gold at the gate for binding alkanethiols,[11] forming an oxide layer for silanization,[3,12] and photopatterning terminal alkenes with UV light.[7] An important requirement with FET biosensors is to have the analyte binding site of the receptor as close as possible to the surface to increase device sensitivity.[13] The disadvantage of the intermediate oxide or gate metallization layers is the increased distance that charged analytes bind to the charge carrier channel resulting in lowered sensitivity. Also, the effectiveness of the UV functionalization method is offset by the limited commercial availability of molecules optimized for the UV binding procedure. An alternative route is to bind receptors to nanostructures patterned at the gate to achieve a high receptor density. This was demonstrated by binding enzymes to ZnO nanorods grown at the gate surface.[14] Further improvement in nanostructure functionalization is possible with deposition of commercially available nanoparticles with linker molecules already attached.

In this work, AlGaN/GaN HEMTs were used as a sensor platform with gold nanoparticles (Au NPs) directly physisorbed to the AlGaN layer. Au NPs provide a well-established system for detection of analyte-receptor interactions that have been used for the detection of various biomolecules including DNA, proteins, and cellular surface receptors.[15] The advantages of using Au NPs to functionalize AlGaN/GaN HEMTs are the straightforward deposition of the NPs, the close proximity of functionalized Au NPs to the underlying charge carrier channel to improve device sensitivity, and the commercial availability of Au NPs functionalized with various receptors. To determine the sensitivity of AlGaN/GaN HEMTs to variations in adsorbed molecules, this study used Au NPs functionalized with three different

a)Author to whom correspondence should be addressed. Electronic mail: ivanisevic@ncsu.edu.

alkanethiol molecules with a terminal chemical group consisting of a methyl, amine, or carboxyl. These different functional groups provided different charge distributions among the three alkanethiol molecules.

The HEMT devices were fabricated on a wafer consisting of 30 nm Si doped $Al_{0.3}Ga_{0.7}N$ on 2.0 μm unintentionally doped GaN grown by metal organic chemical vapor deposition on a sapphire substrate.[16] The Ti/Al/Ni/Au source-drain ohmic contacts were patterned by a liftoff process. Device-to-device isolation was achieved with reactive ion etching using BCl_3 and Cl_2 gases to obtain an etch depth of ~100 nm. The ohmic contacts were rapid thermal annealed at 820 °C for 60 s in nitrogen gas. The Ni/Au gate Schottky contacts were also patterned by a liftoff process. The transistor dimensions were 15 μm channel length, 4 μm gate length, and 100 μm or 50 μm gate width. An illustration of the HEMT structure is shown in Figure 1.

The 30 nm diameter Au NPs were purchased with the following alkanethiols attached: 1-hexanethiol, 6-mercaptohexanoic acid, or 6-amino-1-hexanethiol hydrochloride (Nanopartz Inc.). The HEMTs referred to as "NP treated" were treated by spotting 5 μl of each NP solution on one of three 3 mm × 3 mm device wafers and allowed to air dry. The device wafers were ultrasonicated in deionized (DI) water in a microcentrifuge tube for 5 min to remove loosely adsorbed NPs. The wafers were subsequently rinsed with DI water, dried with nitrogen gas, and either surface potential or electrical measurements were obtained. The NP spotting procedure resulted in submonolayer coverage as viewed with atomic force microscopy (not shown). To distinguish between the effects of the Au NPs and alkanethiols in close proximity to the charge carrier channel, a solution of the same alkanethiol that was bound to the Au NPs on each HEMT was spotted on the NP treated devices to increase the amount of alkanethiol present. Specifically, the HEMTs referred to as "NP-alkanethiol treated" were spotted with 4 μl to 10 μl of 6-mercaptohexanoic acid, 1-hexanethiol, or 6-amino-1-hexanethiol hydrochloride (Sigma Aldrich) diluted to 1 mM in ethanol. The wafers were allowed to air dry and either surface potential or electrical measurements were obtained.

To measure the surface potential difference between the Au NPs and the HEMT surfaces, the scanning Kelvin probe technique was used to collect data from 8 to 20 sample regions from each treatment with a Cypher scanning probe microscope (Asylum Research). Electrical measurements were collected with a Keithley 4200 Semiconductor Characterization System on 11 or 12 HEMTs for each treatment. For drain current (I_D) versus drain-source voltage (V_{DS}) measurements, V_{DS} was swept from 0 to 12 V by 0.05 V steps while the gate voltage (V_{GS}) was either left floating or stepped from 1 to −3 V by −0.5 V steps. HEMTs were compared by using relative ΔI_D, which is defined as $(I_D\text{-}I_{Do})/I_{Do}$ where I_D is the drain current following treatment with NPs or alkanethiol and I_{Do} is the drain current before either treatment. A linear mixed-model analysis of variance was conducted with SAS software (SAS Institute Inc.) to determine if ΔI_D differed significantly when the HEMTs were exposed to the various functional groups and treatments (NP or NP-alkanethiol). Functional group and treatment were considered fixed-effect factors. ΔI_D of the HEMTs was modeled as the sum of overall mean, main effects of functional group and treatment, and the interaction effect between functional group and treatment. Random effects were modeled as the sum of variation among HEMTs (nested within functional groups) and residual variation (modeled as a residual variance for each functional group). Pairwise comparisons between least squares means were used to study differences among significant experimental effects. The Bonferroni correction method for adjusting p values was applied to control for type I error.[17]

Surface potential measurements were collected to measure the influence of the adsorbed Au NPs on the surface potential of the underlying AlGaN. Scanning Kelvin probe microscopy was conducted on areas of the AlGaN/GaN wafers where the Au NPs were spaced far enough apart so that it was possible to measure the surface potential of the NPs compared to the surface potential of the area between NPs. Figure 2 shows that the surface potential of NPs with

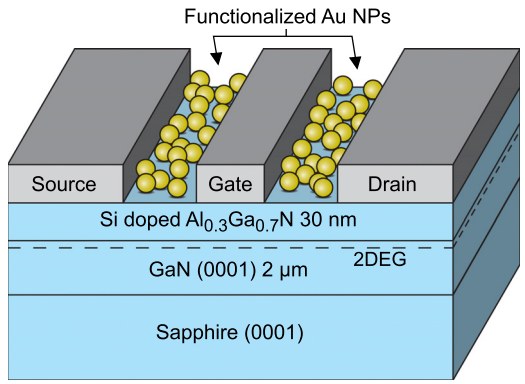

FIG. 1. Diagram of the HEMT structure used in this work. Gold nanoparticles covered all areas of the device wafer and did not specifically adsorb into channels as shown here. The HEMT is not drawn to scale.

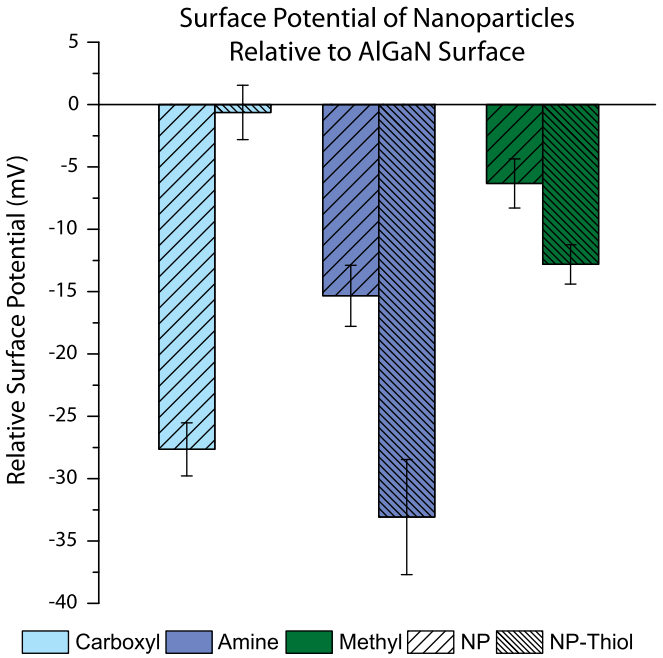

FIG. 2. Surface potential of the Au NPs compared to the AlGaN area surrounding the NPs. Error bars show standard error. NP treated (NP); NP-alkanethiol treated (NP-Thiol).

all three functional groups had a surface potential lower than the surrounding AlGaN surface. The potential across the Au NP to semiconductor (AlGaN) interface is the built-in potential from the Schottky contact at the interface minus the potential due to the charge distribution of the molecular adsorbate (alkanethiols) on the NPs.[18] The Schottky contact results in band bending in the AlGaN near the NPs that likely caused electron depletion on the AlGaN surface, induced a net positive charge in the AlGaN depletion region, and resulted in negative surface potentials on the NPs relative to the positively charged AlGaN surface. One change from NP adsorption to the subsequent alkanethiol adsorption was the near disappearance of a surface potential difference between carboxyl terminated Au NPs and the surrounding area. The 6-mercaptohexanoic acid likely covered the surrounding AlGaN and resulted in surface potential measurements comparing Au NPs covered in 6-mercaptohexanoic acid with a layer of 6-mercaptohexanoic acid over the AlGaN. Additionally, there was an increased magnitude of surface potential difference between amine functionalized Au NPs and the surrounding area following 6-amino-1-hexanethiol hydrochloride deposition. This may have resulted from preferential adsorption of the alkanethiol or HCl salt to the Au NPs or surrounding AlGaN. Importantly, the observed differences in surface potential when comparing different functional groups and treatments provided motivation for using the AlGaN/GaN HEMT system since these HEMTs detect changes in adsorbed surface charge.[2]

Since charged adlayers are able to molecularly gate transistors,[19] it is expected that the greatest sensitivity to adsorbed molecules occurs at the operating point where ΔV_{GS} results in the greatest relative ΔI_D. This is equivalent to finding the maximum value of transconductance (g_m) divided by I_D. Specifically, the most favorable operating point for relative ΔI_D comparisons was determined from the pretreatment I_D-V_{DS} plots where V_{GS} was stepped by finding the values of V_{DS} and V_{GS} that maximized the right side of Eq. (1).

$$\frac{dI_D/dV_{GS}}{I_D} = \frac{(I_{Dn} - I_{Dn-1})/(V_{GSn} - V_{GSn-1})}{0.5(I_{Dn} + I_{Dn-1})}. \quad (1)$$

Based on the maximum values derived from Eq. (1), relative ΔI_D following each treatment was compared for each HEMT at $V_{DS} = 0.5\,V$ and $V_{GS} = -1.5\,V$ or $-2.0\,V$ depending on which value of V_{GS} maximized the right side of Eq. (1) for each HEMT. For each HEMT, these V_{GS} values were near the HEMT threshold voltage (V_t). This result is similar to that previously reported where subthreshold gate voltages gave the greatest relative ΔI_D when the AlGaN/GaN HEMT detected an analyte bound at the gate.[6] Figure 3 shows the values derived from Eq. (1) versus V_{DS} and V_{GS} for a representative HEMT. Additional electrical measurements were obtained to compare relative ΔI_D at $V_{DS} = 0.5\,V$ with the gate electrode floating. The comparison between HEMTs operated with and without a gate bias was important since several AlGaN/GaN HEMT biosensors in the literature were operated without the presence of a biased gate electrode and relied solely on the molecular gating that occurred when analytes bound to the gate surface.[8,11,12]

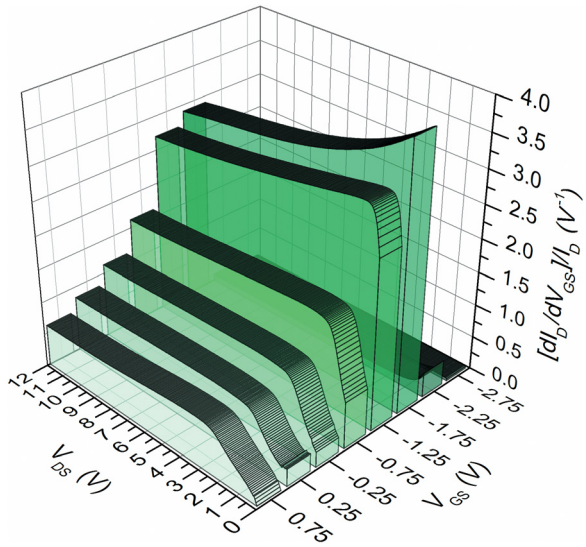

FIG. 3. $(dI_D/dV_{GS})/I_D$ versus V_{DS} and V_{GS} for a representative HEMT prior to NP or alkanethiol treatments. For this HEMT, the operating point that gives the greatest relative ΔI_D for ΔV_{GS} is near $V_{DS} = 0.5\,V$ and $V_{GS} = -1.5\,V$.

Figure 4 displays the results of the statistical analysis of relative ΔI_D for three sets of HEMTs that were either NP treated or NP-alkanethiol treated. Each set was spotted with one of the three types of functionalized Au NPs used in this experiment followed by physisorption of the respective alkanethiol. The statistical comparisons included comparing each

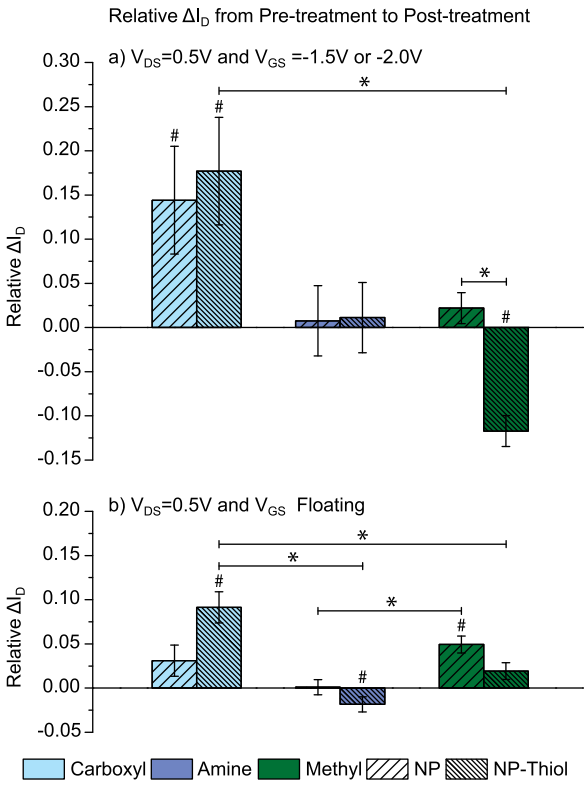

FIG. 4. (a) Relative ΔI_D with V_{DS} and V_{GS} biased near the optimal operating point. (b) Relative ΔI_D with V_{GS} floating. Asterisks show statistically significant differences. Pound symbols indicate value is significantly different from 0. For both cases, $p < 0.05$. All values are relative to pretreatment I_D at the specified bias. Least squares means are displayed with error bars showing standard error. The calculated least squares means were the same as the observed means. NP treated (NP); NP-alkanethiol treated (NP-Thiol).

relative ΔI_D value to zero, comparing values between NP treated and NP-alkanethiol treated within each functional group, and comparing each functional group within treatments (NP or NP-alkanethiol). In all cases, significance was declared for $p < 0.05$.

In Figure 4(a), relative ΔI_D is shown for each treatment near the optimal operating point. The NP treated and NP-alkanethiol treated HEMTs had a positive relative ΔI_D for the carboxyl functional group while the NP-alkanethiol treated HEMTs with the methyl functional group had negative relative ΔI_D. The remaining treatments resulted in negligible relative ΔI_D for the biased gate measurements. When comparing relative ΔI_D among the NP treated HEMTs, the null hypothesis that the three functional groups resulted in three equal values was not rejected. However, the comparison of relative ΔI_D for the NP-alkanethiol treated HEMTs revealed a significant difference between the carboxyl and methyl functional groups. The only significant difference between NP treated and NP-alkanethiol treated within each functional group was for the methyl functional group where relative ΔI_D decreased with alkanethiol adsorption.

In Figure 4(b), the effect on relative ΔI_D is shown for each treatment for the same devices tested in Figure 4(a) except that the gate was floating rather than biased. The NP treatment with the methyl functional group and the NP-alkanethiol treatment with the carboxyl functional group both caused positive relative ΔI_D. In contrast, the NP-alkanethiol treatment with the amine functional group caused a negative relative ΔI_D. The remaining treatments resulted in insignificant relative ΔI_D. When comparing the NP treatments, there was a significant difference between the amine and methyl functional groups. The relative ΔI_D comparison among the NP-alkanethiol treatments revealed significant differences between the carboxyl functional group compared to both the amine and methyl functional groups. No significant differences existed between NP treatment and NP-alkanethiol treatment within each functional group category.

There are three important points to discuss when comparing Figures 4(a) and 4(b). First, it is important to address the apparent change in relative ΔI_D polarity of amine NP-alkanethiol treatment and methyl NP-alkanethiol treatment depending on whether the gate was biased or floating. The discrepancy is attributed to random error since one value from each pair is not significantly different from zero. For example, the methyl NP-alkanethiol treatment had a negative value when biased, but the positive value for the floating state was not significantly different from zero. Second, for most of the treatments, relative ΔI_D was larger when the HEMT gate was biased near the optimal operating point than when the gate was floating. For HEMTs that detect analyte binding while submerged in electrolytic solutions, an electrolyte gate electrode or an insulated gate electrode covering only a portion of the area over the channel will likely bias the transistor into its most sensitive operational region to optimize device sensitivity. Third, and most importantly, there exists a significant difference between the carboxyl NP-alkanethiol treatment and the methyl NP-alkanethiol treatment for both biased and floating V_{GS}. This fact demonstrates that it was possible to detect differences in terminal functional groups when enough alkanethiol molecules were physisorbed at the gate surface. Possible reasons for differences in relative ΔI_D based on functional groups include different surface charges due to partial/complete protonation or deprotonation,[19] differential stacking of molecules resulting in multilayers of deposited alkanethiol, and disordered molecular layer formation resulting in a net dipole that molecularly gates the transistor.[20]

It is important to note the advantages and disadvantages of AlGaN/GaN HEMT functionalization by Au NP adsorption. One advantage is that there is no risk of forming multilayers of receptors on the Au NPs since the surfaces are functionalized under controlled conditions by the commercial vendors. Without multilayers, the detection time is decreased due to eliminating the time required for analytes to diffuse through multilayers of receptors.[21] Another advantage is the commercial availability of functionalized Au NPs and the straightforward method of spotting NPs on a device wafer. On the other hand, one disadvantage of HEMT functionalization by adsorption of Au NPs is the difficulty of controlling the surface concentration of NPs. In this work, surface concentrations were variable within wafers and between wafers with different NP functionalizations. An additional disadvantage is that the AlGaN layer is not protected from oxidation. However, growth of a thin ~ 2 nm GaN cap on the AlGaN layer easily remedies this problem.[4]

To demonstrate the detection of a biological analyte, a proof-of-concept nonspecific DNA detection experiment was performed. DNA was expected to noncovalently bind to amine-terminated Au NPs due to both hydrogen bonds between the nucleotides and the surface functional group as well as electrostatic bonds between the negatively charged DNA backbone and the positively charged amine-terminated surface.[22] Two wafers with 12 HEMTs each were prepared with amine-terminated Au NPs as described earlier, and the optimal operating point was found for each HEMT at $V_{DS} = 0.5$ V and $V_{GS} = -2.0$ or -2.5 V. One wafer was soaked in PBS (phosphate buffered saline) for 15 h then soaked in a solution of 50 μM synthetic 20-mer DNA in PBS for 15 h. The second wafer was soaked in PBS for 30 h. The wafers were rinsed with DI water and dried. The relative ΔI_D at the optimal operating point was calculated as I_D change after soaking in PBS or DNA solutions divided by I_D after NP deposition. The relative ΔI_D means and standard errors were -0.15 +/− 0.03 for the DNA exposed HEMTs and 0.05 +/− 0.02 for the PBS exposed HEMTs. The values are significantly different with a p-value of 3.2×10^{-5} as determined by the Kruskal-Wallis test.[23] The negative relative ΔI_D for the DNA experiment is attributed to decreased electron concentration in the channel due to band bending caused by the negative charge on the DNA backbone. The smaller magnitude of relative ΔI_D for the PBS control experiment is likely caused by residual salt deposition on the surface.

In conclusion, functionalized Au NPs were adsorbed to the surface of AlGaN/GaN HEMTs to demonstrate electrical detection of functional group differences on the adsorbed NPs. The most sensitive operational region for detecting relative ΔI_D with NP adsorption was where V_{GS} was biased near V_t. The different functional groups had differing effects on molecularly gating the HEMTs due to variations in charge distribution that were observable by scanning Kelvin probe

microscopy. Applications of the NP/HEMT system include detection of analytes such as specific DNA sequences, proteins, or other metabolites by deposition of Au NPs functionalized with biological receptors onto AlGaN/GaN HEMTs. In sensors with arrays of biochemical sensing transducers, incorporation of statistical analysis methods on-chip could help reduce false positives and negatives when device-to-device variability exists.

This work was supported by NSF under CMMI-0856391, NIH/NCRR-Indiana Clinical and Translational Sciences Institute—TL1 Program under TL1 RR025759 (A. Shekhar, PI), and the Indiana University Medical Scientist Training Program under NIH GM077229. M.G. was supported as an REU participant by NSF (EEC 1156762).

[1]M. Curreli, R. Zhang, F. N. Ishikawa, H. K. Chang, R. J. Cote, C. Zhou, and M. E. Thompson, IEEE Trans. Nanotechnol. **7**(6), 651 (2008); C. B. Jacobs, M. J. Peairs, and B. J. Venton, Anal. Chim. Acta **662**(2), 105 (2010); S. Myung, P. T. Yin, C. Kim, J. Park, A. Solanki, P. I. Reyes, Y. Lu, K. S. Kim, and K. Lee, Adv. Mater. **24**, 6081 (2012).
[2]B. S. Kang, H. T. Wang, F. Ren, and S. J. Pearton, J. Appl. Phys. **104**(3), 031101 (2008).
[3]S. Gupta, M. Elias, X. J. Wen, J. Shapiro, L. Brillson, W. Lu, and S. C. Lee, Biosens. Bioelectron. **24**(4), 505 (2008).
[4]A. Podolska, S. Tham, R. D. Hart, R. M. Seeber, M. Kocan, M. Kocan, U. K. Mishra, K. D. G. Pfleger, G. Parish, and B. D. Nener, Sens. Actuators B **169**, 401 (2012).
[5]S. A. Jewett, M. S. Makowski, B. Andrews, M. J. Manfra, and A. Ivanisevic, Acta Biomateria. **8**(2), 728 (2012).
[6]X. Wen, S. Gupta, Y. Wang, T. R. Nicholson, S. C. Lee, and W. Lu, Appl. Phys. Lett. **99**(4), 043701 (2011).
[7]S. U. Schwarz, S. Linkohr, P. Lorenz, S. Krischok, T. Nakamura, V. Cimalla, C. E. Nebel, and O. Ambacher, Phys. Status Solidi A **208**(7), 1626 (2011).
[8]Y. L. Wang, B. H. Chu, K. H. Chen, C. Y. Chang, T. P. Lele, G. Papadi, J. K. Coleman, B. J. Sheppard, C. F. Dungen, S. J. Pearton, J. W. Johnson, P. Rajagopal, J. C. Roberts, E. L. Piner, K. J. Linthicum, and F. Ren, Appl. Phys. Lett. **94**(24), 243901 (2009).
[9]G. Steinhoff, B. Baur, G. Wrobel, S. Ingebrandt, A. Offenhausser, A. Dadgar, A. Krost, M. Stutzmann, and M. Eickhoff, Appl. Phys. Lett. **86**(3), 033901 (2005).
[10]A. Podolska, M. Kocan, A. M. G. Cabezas, T. D. Wilson, G. A. Umana-Membreno, B. D. Nener, G. Parish, S. Keller, and U. K. Mishra, Appl. Phys. Lett. **97**(1), 012108 (2010).
[11]B. H. Chu, C. Y. Chang, K. Kroll, N. Denslow, Y. L. Wang, S. J. Pearton, A. M. Dabiran, A. M. Wowchak, B. Cui, P. P. Chow, and F. Ren, Appl. Phys. Lett. **96**(1), 013701 (2010).
[12]B. S. Kang, F. Ren, L. Wang, C. Lofton, W. W. Tan, S. J. Pearton, A. Dabiran, A. Osinsky, and P. P. Chow, Appl. Phys. Lett. **87**(2), 023508 (2005).
[13]J. P. Kim, B. Y. Lee, S. Hong, and S. J. Sim, Anal. Biochem. **381**(2), 193 (2008).
[14]B. H. Chu, B. S. Kang, F. Ren, C. Y. Chang, Y. L. Wang, S. J. Pearton, A. V. Glushakov, D. M. Dennis, J. W. Johnson, P. Rajagopal, J. C. Roberts, E. L. Piner, and K. J. Linthicum, Appl. Phys. Lett. **93**(4), 042114 (2008); B. S. Kang, H. T. Wang, F. Ren, S. J. Pearton, T. E. Morey, D. M. Dennis, J. W. Johnson, P. Rajagopal, J. C. Roberts, E. L. Piner, and K. J. Linthicum, Appl. Phys. Lett. **91**(25), 252103 (2007).
[15]M. C. Daniel and D. Astruc, Chem. Rev. **104**(1), 293 (2004).
[16]S. Mita, R. Collazo, A. Rice, J. Tweedie, J. Q. Xie, R. Dalmau, and Z. Sitar, Phys. Status Solidi C **8**(7–8), 2078 (2011).
[17]R. C. Littell, G. A. Milliken, W. W. Stroup, R. D. Wolfinger, and O. Schabenberger, *SAS for Mixed Models*, 2nd ed. (SAS Institute, Cary, NC, 2006).
[18]V. Dobrokhotov, D. N. McIlroy, M. G. Norton, A. Abuzir, W. J. Yeh, I. Stevenson, R. Pouy, J. Bochenek, M. Cartwright, L. Wang, J. Dawson, M. Beaux, and C. Berven, J. Appl. Phys. **99**(10), 104302 (2006).
[19]O. Shaya, I. Amit, H. Einati, L. Burstein, Y. Shacham-Diamand, and Y. Rosenwaks, Appl. Surf. Sci. **258**(8), 4069 (2012).
[20]O. Shaya, H. Einati, N. Fishelson, Y. Shacham-Diamand, and Y. Rosenwaks, Appl. Phys. Lett. **97**(5), 053501 (2010).
[21]B. Baur, J. Howgate, H. G. von Ribbeck, Y. Gawlina, V. Bandalo, G. Steinhoff, M. Stutzmann, and M. Eickhoff, Appl. Phys. Lett. **89**(18), 183901 (2006).
[22]D. R. Call, D. P. Chandler, and F. Brockman, BioTechniques **30**(2), 368 (2001); H. Y. Wang, R. L. Malek, A. E. Kwitek, A. S. Greene, T. V. Luu, B. Behbahani, B. Frank, J. Quackenbush, and N. H. Lee, Genome Biol. **4**(1), R5 (2003).
[23]D. C. Montgomery, *Design and Analysis of Experiments*, 7th ed. (Wiley, 2009).